An investigation into pressure drop through bends in pneumatic conveying systems

Atul Sharma and S. S. Mallick

Laboratory for Particle and Bulk Solids Technologies, Department of Mechanical Engineering, Thapar Institute of Engineering and Technology, Patiala, India

1. Introduction

Pneumatic conveying is the process of conveying bulk solids using a gas as the transport medium through pipes. Pneumatic conveying offers many advantages over alternative mechanical conveying systems, such as dust-free transportation, relatively high levels of safety, low routine maintenance and manpower costs, layout flexibility and ease of automation, thereby making it suitable for a variety of industrial use. Some of the industries in which bulk materials are conveyed include agriculture, power plant, cement, mining, chemical, pharmaceuticals, paint manufacture, metal refining and processing (McGlinchey 2008). Designing a pneumatic conveying system include determining the minimum transport boundary and total pipeline pressure drop as key parameters. Incorrect estimation of these parameters may results in serious operating problems such as more power consumption, system wear, line blockage, inadequate throughput and product degradation (Molerus 1996; Wypych 1999). Hence an accurate prediction of these parameters is required for smooth, trouble free and optimum working of the pneumatic conveyor. In a pneumatic conveying system, the total pipeline pressure drop comprises of four components, that is, losses in straight pipe, bend, vertical and losses due to the initial acceleration (Mallick 2009). For a typical industrial system, horizontal straight pipe and bend losses are more critical areas of concern as they form the significant share of total pipeline drops.

Over the last two decades relatively more efforts have been made towards understanding the flow mechanism and modeling of pressure drop for straight pipes (Mallick 2009; Setia et al. 2016) than bends. Conveying through a bend involves vortex flow, direction and momentum change of particles and gas, reacceleration at its exit and may even cause phase separation (Venkatasubramanian et al. 2000). Flow through bends also results in a roping phenomenon where most of the moving particles are concentrated into a small portion of the cross-sectional area of the pipe due to centrifugal forces (Yan, Byrne, and Coulthard 1994). A combination of these phenomenon, occurring simultaneously, make it difficult to model the pressures drop and flow situation (Bilirgen and Levy 2001).

There exist some models for bend pressure drop, such as Schuchart (1968), Singh and Wolfe (1972), Rossetti (1983), Chambers and Marcus (1986), Westman, Michaelides, and Thomson (1987), Pan (1992), Pan and Wypych (1998). More recent models include that of Chunhui et al. (2012) and Cai et al. (2014). These models are generally empirical based, that is, they depend on the specific properties of test materials and developed under a range of flow and pipeline/ bend conditions. Because the total pipeline pressure drop depends on both the straight pipe and bend losses, therefore it is important to examine the effect of choosing different bend loss prediction models (while keeping the same model for solids friction factor for straight pipes). The objectives of

A	Blow Tank
B	Receiver Bin
C	Bag Filter
D	Compressed Air
B1–B6	90°Bends
B1	Location 1 Test Bend (R_b = 1.0/0.8/0.6 m)

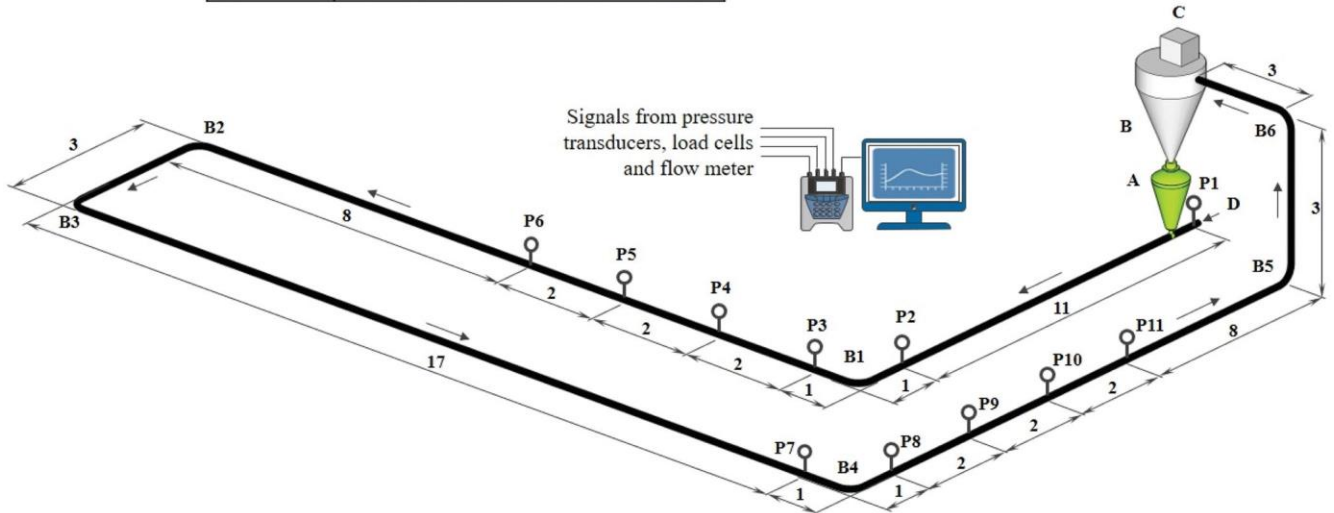| B4	Location 2 Test Bend (R_b=1 m)
P1–P11	Pressure Transducers
Pipe Diameter	42/53 mm
Loop Length	69 m
All dimensions shown in the figure are in meters	

Figure 1. Schematic layout of test rig with 42/53 mm I.D. 69 m length having test bends.

this paper are (1) to investigate into the effect of selection of bend model (to predict bend loss) on the total pipeline pressure drop and (2) to carry out comprehensive test program to generate large data set (for bend loss for different products/pipeline diameters and locations of test bend in pipeline) for developing new accurate bend loss model for reliable prediction of pressure drop through the bends.

2. Experimental work

Pneumatic conveying test facility has been developed at Thapar Institute of Engineering and Technology, Patiala (India). A typical schematic of the test setup used is shown in Figure 1. Kirloskar made electric-powered Model KES 18-7.5 rotary screw compressor was used having the capacity of 3.37 m³/min of free air delivery and maximum delivery pressure of 750 kPa. Air flow control valve was installed in the compressed air line upstream of the blow tank to vary the conveying air flow rates over a wide range of air flows. A vortex flow meter was installed in the compressed air line for the measurement of air flow rates. Bottom discharge type blow-tank of capacity 0.2 m³ capacity of water fill volume was used to feed bulk solids into the pipeline in pressure conveying. The blow tank was mounted with solenoid operated dome-type material inlet, outlet and vent valves. A receiver bin of 0.7 m³ capacity was installed on top of the blow tank and was fitted with bag filters having pulse jet type cleaning mechanism. The blow tank and receiver bin were supported by shear beam type load cells to measure solids flow rates. Two mild steel pipelines of 43 mm I.D 69 m length and 54 mm I.D 69 m length were used as the test pipelines. The test loops included a 3 m vertical lift and 5 90 bends having 1 m radius of curvature in addition to a test

bend. Various static pressure measurement points were installed along the pipeline across bends, where P1 transmitter was used to measure the total pipeline pressure drop. P2 to P6 transmitters and P7 to P11 transmitters were used in test bend locations 1 and 2, respectively (see Figure 1). P2 and P7 were used to measure pipeline static pressures just at the beginning of bends, whereas P3 to P6 and P8 to P11 were used to measure static pressure after bends at 2-m interval distance from each other (to capture losses at the bend and just after the bend caused by reacceleration of powders). Specification of static pressure transducers: manufacturer: Endress & Hauser, model: Cerabar PMC131, pressure range: 0–2 bar, maximum pressure: 3.5 bar (absolute), current signal: 4–20 mA. Analog electric output from the pressure transducers (4–20 mA) and load cells (0–5 V) were acquired and digitized at sampling frequency 50 Hz with the help of multi-channel data acquisition system having 16-bit resolution. Such sampling frequency ensures new separate reading per second for each of pressure transmitters. All other required instruments such as PRV (pressure reducing valve), flow meter, NRV (nonreturn valve), blow valve, pressure gauge and load cells (shear beam type) were suitably placed. Calibration of the pressure transducer, load cells and flow meter were performed using a standardized calibration procedure (Mallick 2009; Setia et al. 2016). To record the electrical output signals from the load cells, pressure transducers and flow meter, a portable PC compatible data logger was used. The data logger had 16 different channels with 14 bit resolution. Gray cement, fly ash and white cement were used in the test program. These powders were conveyed through two different pipeline (or bend) diameters: 53 and 42 mm, respectively. Two test

locations were used: B1 bend and B4 bend locations (Figure 1). Three different radius of curvature of bends were used: 1000, 800 and 600 mm. As regards location of transmitters before and after the bend, Tripathi, Levy, and Kalman (2018), Hall (2012) and Akilli, Levy, and Sahin (2001) suggested that the initial acceleration length or the minimum straight length required for the powders to achieve developed flow (or steady flow condition is 30 D, where D is the inner diameter of pipeline). In the experimental setup, the first pressure transmitter in solid-gas line is located after 200 D from the product feed point. Regarding reacceleration length after the bend, the work of previous researchers, such as Levy and Mason (1998), Hettiaratchi, Woodhead, and Reed (1998), Hyder et al. (2000), Hastie et al. (2001), Maynard (2006) and Vasquez et al. (2008), suggested that the reacceleration length after the bend varies from 30 D to 100 D and 2 m to 5 m. The maximum reported length is 5 m till which transient effects have been reported. Nonetheless, the effects of transients

were verified using an established technique mentioned in Pan (1992). Based on above, location of the first transmitter after 11 m from the blow tank and measurement of static pressure after up to 6 m of the test bend were considered appropriate. Measurement of static pressure for highly concentrated fluidized dense-phase flow of fine powders is a challenging task due to large signal fluctuations. To address this, some of the experiments were repeated and filters attached to pressure transmitter were cleaned and the transmitters were recalibrated periodically to ensure accuracy of data. Physical properties of the products are provided in Table 1. Details of different combinations of choice of products, pipe (or bend) diameters, test bend locations and radius of curvature of bends are provided in Table 2.

In addition to the test data obtained from Thapar Institute for Engineering and Technology (Patiala), additional test data were also used from the pneumatic conveying test facility of

Table 1. Physical properties of powder conveyed.

Product	d_{10} (mm)	d_{50} (mm)	d_{90} (mm)	q_b (kg/m³)	q_p (kg/m³)
Gray Portland Cement	3	18	53	1020	2680
White Portland Cement	3	19	50	1028	2720
Fly Ash	9	65	206	884	2000

Table 2. Different bend locations, and products. bend radius of curv atures, bend diameters

Case no.	Product	R_b (mm)	D (mm)	R_b/D	Location
1	Gray Portland cement	600	53	11	B1
2	Gray Portland cement	800	53	15	B1
3	Gray Portland cement	1000	53	19	B1
4	Gray Portland cement	1000	53	19	B4
5	Fly ash	1000	53	19	B1
6	White Portland cement	1000	53	19	B1
7	White Portland cement	1000	42	24	B1

University of Wollongong, Australia. Power station fly ash was conveyed from dilute phase to fluidized dense phase through 69mm ID 168m long and 105mm ID 168m long pipelines. A schematic of the test set-up for the 69mm ID 168m long pipeline (for fly ash) is shown in Figure 2. Physical properties of this fly ash is provided in Table 3.

The test set-up consists of tandem 0.9 m³ bottomdischarge type blow tank feeding system. Pipes and bends used in the pilot plant were made of mild steel material. The pipeline includes 7 m vertical lift, five 1 m radius of curvature and 90 angle bends, and 150 mm N.B. tee-bend

Table 3. Physical properties of the fly ash conveyed.

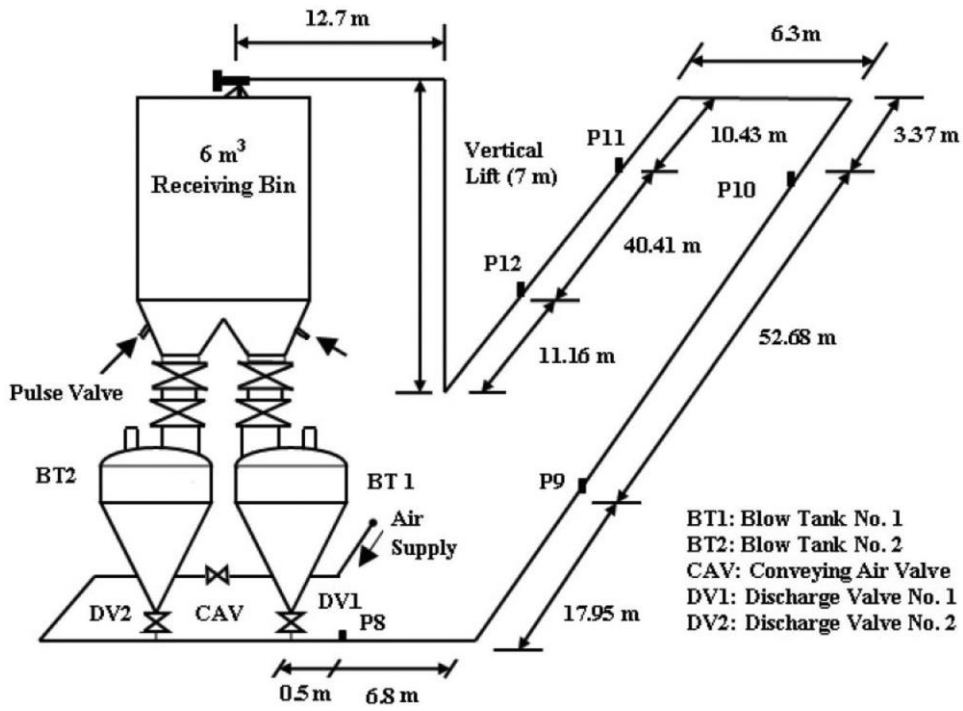| d_{10} (mm)	d_{50} (mm)	d_{90} (mm)	q_s (kg/m³)	q_b (kg/m³)	D (mm)	L (m)
5	30	145	2300	700	69	168

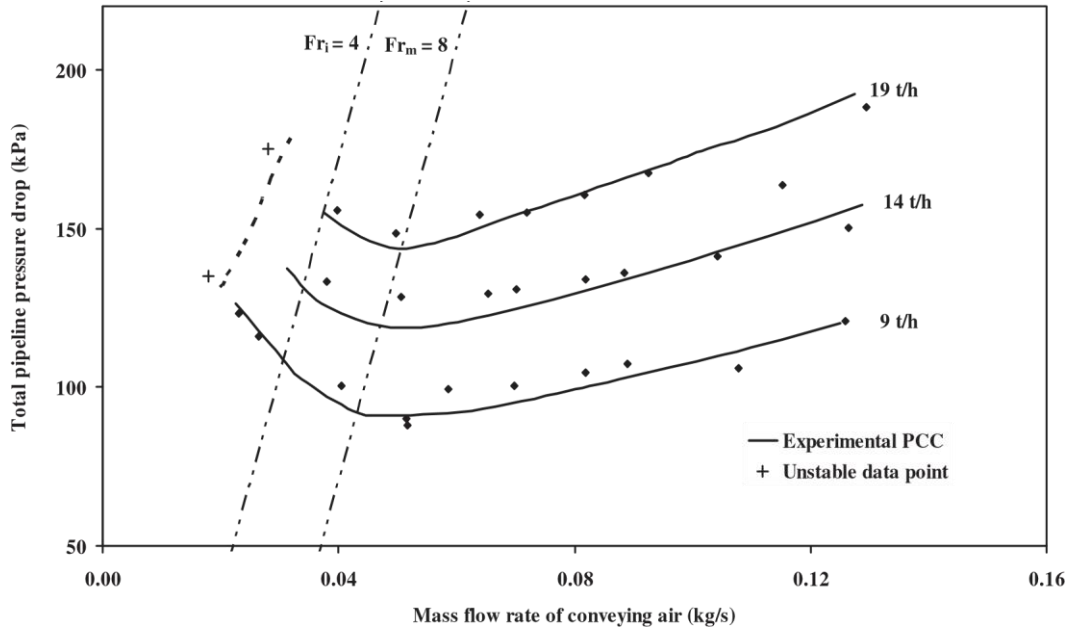Figure 2. Layout of the 69 mm I.D. x 168 m test rig (for fly ash).

Figure 3. Experimental pneumatic conveying characteristics for total pipeline pressure loss for fly ash and 69 mm I.D. 168 m pipe.
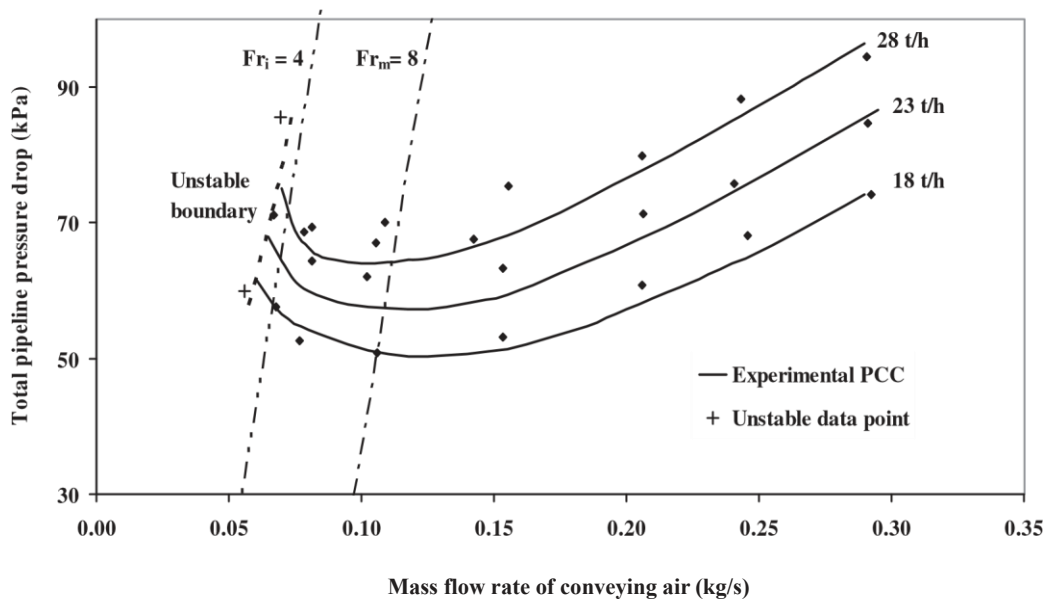
Figure 4. Experimental pneumatic conveying characteristics for total pipeline pressure loss for fly ash and 105 mm I.D. 168 m pipe.

connecting the end of the pipeline to the feed bin or receiver bin. A receiving bin with insertable pulse jet dust filter of capacity 6 m³ was installed on the top of the blow tank. In order to supply the compressed air at a maximum pressure of approximately 800 kPa-g, Ingersoll Rand diesel powdered Model P375-WP, 10.6 m³/min free air delivery screw compressor was used. To measure static pressure in the horizontal straight sections of pipeline, five static pressure transducers were employed along all the pipelines, i.e. P8, P9, P10, P11, P12. The static pressure transducers had the following specification: manufacturer: Endress and Hauser, model: Cerabar PMC133, pressure range: 0–6 and 0–2 bar-g, maximum pressure: 40 bar (absolute), current signal: 4 to 20 mA. The P8 transducer was used to measure the total pipeline pressure drop, whereas P9–P12 tapping points were installed to provide "straight pipe" pressure loss data along the pipeline. A portable PC compatible data logger (Datataker 800 or DT800 of Data electronics) was used to record the electrical output signals from the load cells, pressure transducer and flow meters. Figures 3 and 4 show experimental Pneumatic Conveying Characteristics (PCC) for fly ash conveyed through the 69 mm ID 168 m long and 105 mm ID 168 m long pipelines (Mallick 2009) with experimental data points superimposed. These characteristics have been used in this study to evaluate the effect of bend models on the predicted total pipeline pressure losses.

3. Bend pressure drop models

An early comprehensive study of pressure drop caused by bends was done by Schuchart (1968) using glass (1500–3000 mm, 2610 kg/m³) and plastic (2180 mm, 1140 kg/ m³) as the test materials (Klinzing et al. 2010). A wide range of bend radius of curvature ranging from 60 mm to 350 mm and pipe I.D: 34.35 mm, were

explored and the solids contribution of the pressure drop due to solids-gas flow through a bend was expressed as

$$Dp_{bs} \, 2R_{b\ 1:15} \, Dp_{zs} \, \tfrac{1}{4} \, D$$

$$210(1)$$

where Dp_{bs} is the bend pressure drop due to the solids only, Dp_{zs} is the pressure drop due to the solids for an equivalent length of straight pipe (having the same length as the arc length of the bend), and R_b is radius of curvature of the bend.

Singh and Wolfe (1972) used dimensional analysis to model the bend pressure drop (Pan 1992). They conveyed granular material through bends of different radius of curvature (381, 762 and 1220 mm) all having the internal diameter of 150 mm. They conducted 108 experiments and expressed the seven important variables in the following dimensionless ratios:

$$\frac{}{D_2} \quad \frac{}{a!} \quad \frac{q_{fo}V_{bfo2} \, \tfrac{1}{4} \, RD_b \, q_{fo}Vm_{fos}}{(2) \, Dp} \\ f \quad , \quad , b$$

where b_a is bend angle. It was assumed that a generalized power function law would be valid; a relationship was developed between $q_{DfopV_{bfo2}}$ and $q_{foVm_{fos} \, D2}$, resulting in the following model for bend pressure drop:

$$Dp_b \, \tfrac{1}{4} \, a_c \, þ \, a_s \quad \frac{m_sV_{fo} \quad R_b \quad ab}{D_2 \quad D} \qquad (3)$$

where a_c represents the bend pressure loss under air-only conditions. Using least square method and large number of experimental data, the following expression was obtained:

$$m_s{:}V_{fo} \qquad R_{b\ 0:18}$$

$$Dp_b \frac{1}{4} 0{:}13 \, \flat \, a_s \, \overline{} \, D_2 \, D \qquad (4)$$

Chambers and Marcus (1986) proposed a correlation for predicting pressure loss in bends. The correlation is given as follows

$$Dp_b \frac{1}{4} B\eth 1 \, \flat \, m\text{Þ} \frac{q_f \, V_{f2}}{2} \qquad (5)$$

The bend loss coefficient B depends on the ratio of bend radius of curvature to pipe diameter (Crowe 2005). In the absence of experimental data, Chambers and Marcus (1986) recommend the use of the values given in Table 4.

Das and Meloy (2002) studied the pressure drop in a close-coupled double bend (0.762 m apart) in pneumatic conveying of fly ash. Six different fly ash samples with median particle size ranging from 45–75 mm, particle density and loose poured bulk density ranging from 1938–2499 kg/ m³ and 529–1121 kg/m³, respectively were tested. The bends used in the loop (169.8 m) had the internal diameter of 65.3 mm with a radius of curvature of 158.75 mm. Pressure drops across close-coupled bends were compared to the isolated single 90 bend. The following correlation was derived

Table 4. Bend constant "B" or various bends.

$\frac{R_b}{D}$	B
2	1.5
4	0.75
6	0.50

for the purpose of comparison between the single and closecoupled bends:

$$\frac{Dp_s}{m} \frac{1}{4} X_1 {:} V_b^{X_2} \qquad (6)$$

where X_1 and X_2 are constants specified for a particular ash and bend geometry: for single (Isolated) bends: $X_1 \frac{1}{4} 0.3 \; 10^7$, $X_2 \frac{1}{4} 3.4$ and for double (close-coupled) bends: $X_1 \frac{1}{4} 2.2 \; 10^7$, $X_2 \frac{1}{4} 3.0$.

Chunhui et al. (2012) conducted dense phase pneumatic conveying experiment on rice husk powder and two blendings of the rice husk blended with coal (mass ratio of rice husk to coal ¼ 3:0, 2:1 and 1:2) at the pressure of up to 4.0 MPa. The particle density and mean particle size of these three bulk materials were 1015, 1144, 1272 kg/m³ and 67.81, 65.21, 62.61 mm, respectively. The conveying pipeline (vertical section and horizontal section, as well as the bend) used was made of a smooth stainless steel tube with an internal diameter of 10 mm and a length of about 53 m. The solid pressure drop for the bend was given by:

$$\frac{1}{4} k_{bs} \flat \, R_b \, q_f \, V_{f2} \, (7) \; Dp_{bs} \, m$$

$$\overline{2D} \qquad 2$$

The following correlation was derived for solid friction factor of rice husk conveying through a bend:

$$k_{bs} \frac{1}{4} \eth \, \text{Þe} \; 3{:}41 \; \eth Fr\text{Þ}0{:}66 \; q_{s+30} \quad (8) \; q_f$$

Solid friction factor for coal conveying through a bend was given by:

$$k_{bs} \frac{1}{4} \eth \, \text{Þe} \; 7{:}46 \; \eth Fr\text{Þ}0{:}91 \; q_{s+95} \quad (9) \; q_f$$

Cai et al. (2014) studied the effect of material property, bend geometry and location on pressure drop due to bends in dense-phase pneumatic conveying. They conveyed petroleum coke (two types: mean diameter of 163 lm and 56.69 lm, and bulk density of 616 kg/m³ and 475 kg/m³ respectively) and anthracite powder (two types: mean diameter of 139.9 lm and 52.78 lm, and a density of 736 kg/m³ and 588 kg/m³, respectively) using nitrogen as the conveying gas. Their conveying pipeline was composed of straight pipes and bends made of a smooth stainless pipe with an inside diameter of 10 mm and a total length of 35 m. Three different orientations of bends were examined: vertical downward, horizontal bend, and the vertical upward bend. For horizontal bends, three radius of curvatures (120 mm, 200 mm and 300 mm) were examined. Using Barth's additional pressure theory (pressure drop is considered as the sum of gas and solid pressure drop components) and multivariable linear regression, they derived the empirical correlations of pressure drop through the bend. The bend pressure drop due to solids is given by:

$$Dp_{bs} \; \frac{1}{4} \; 0{:}5 \, m \quad \frac{k_{bs}\flat \, R_b \, q_f}{D} \; V_{f2} : \frac{}{2} \qquad (10)$$

where

$$k_{bs} \frac{1}{4} \eth \, \text{Þe} \; 0{:}126 \; \eth m\text{Þ}0{:}961 \; \eth Fr\text{Þ}0{:}9647 \; d_p \; \frac{0{:}072}{D} \; R_b \frac{0{:}634}{D}$$
$$(11)$$

Rossetti (1983) performed experiments using coarse and fine particles for different bends (bend diameter to pipe diameter ratio 2 to 8.4) and provided Equation (12) for bend pressure loss. He observed that frictional pressure loss for the fine particles is caused by the sliding motion of the particles around the bend walls. These particles get re-accelerated by taking the kinetic energy from the conveying gas. On the other hand, wall collisions are responsible for the energy loss of the coarser particles, resulting less re-acceleration energy losses.

$$q_{fo} V_{fo2}$$

$$\Delta p_b \frac14 k_{bf} \flat k_{bs} \qquad (12)$$

where k_{bf} accounts for the pressure drop due to the air in bend, while k_{bs} accounts for the pressure drop due to solids in bend.

Westman, Michaelides, and Thomson (1987) conveyed four polymers with bulk densities ranging from 572 to 824 kg/m^3, particle densities from 877 to 1320 kg/m^3 of equivalent particle diameter from 3.40 to 3.51 mm using a vacuum system. They studied the bend pressure loss in dilute-phase flow through 90 bends of various geometries (2 R_b/D ¼ 3, 10, 24). They concluded that total pressure loss due to bend can be expressed as a sum of air and solids only pressure drop. The correlation is given as follows:

$$0\frac{\Delta p_b}{:5 q_f V_{f2}} \frac14 k_{Total} \frac14 k_{bf} \flat k_{bs} \qquad (13)$$

$$k_{bf} \frac14 0:167 \left[1 \flat 17:062 \left(2R_b \frac{D}{1:219} \right) \# Re^{0:17} \left(\frac{2R_b}{D} \right)^{0:84} \right] \qquad (14)$$

$$k_{bs} \frac14 \frac{5:4\, m_{1:293}}{Fr_{0:84}\, 2DR_b}\, 0:39 \qquad (15)$$

This model has also assumed that condition at the exit to the bend is more important due to the slowing down of particles at the outlet of bends (because of particle friction against the bend wall) and the subsequent energy requirement to reaccelerate the particles.

Pan (1992) tried to improve the scale-up procedures for the design of pneumatic conveying systems. Based on mathematical and dimensional analysis, semi-empirical correlations were derived predicting the solids friction through bends. He performed experiments on five type of bends: one blinded-tee and four radius bends (R_b: 100, 254, 450 and 1000 mm), and used fly ash as the conveying material with properties: q_s: 2197 kg/m^3; q_b: 634 kg/m^3; mean d_p: 15.5 mm.

In order to investigate into the bend pressure drop, he used a test bend between two long horizontal straight pipes sections. By "minimizing the sum of squared errors", Pan (1992) derived the following bend model:

$$\Delta p_{bs} \frac14 0:5\, m k_{bs} q_{fo}\, V_{fo2} \qquad (16)$$

where

$$k_{bs} \frac14 Y_1\, ðmÞ_{Y2}\, ðFrÞ_{Y3} \qquad (17)$$

Based on his empirical data, Pan (1992) proposed the value of Y1, Y2 and Y3 (for 90 bend angle) as 0.0052, 0.49 and 1.1182 respectively.

Pan and Wypych (1998) derived a bend pressure loss model by conveying four different fly ash samples with median particle size ranging from 3.5–58 mm, particle density and loose poured bulk density ranging from 2180–2540 kg/m^3 and 634–955 kg/m^3, respectively. The model was derived for a wide range of flow conditions (estimated air velocity range at pipe inlet: 3–25 m/s). The bend pressure loss due to solids only is expressed as:

$$\Delta p_{bs} \frac14 0:5\, m k_{bs} q_{fo}\, V_{fo2} \qquad (18)$$

where $k_{bs} \frac14 0:0097\, ðmÞ_{0:5676}\, ðFrÞ_{0:9647}\, ðq_{fo}Þ_{0:6232}$ (19)

4. Effect of bend pressure loss on total pipeline pneumatic conveying characteristics

From the straight pipe data obtained from P11-P12 static pressure measurements for a wide range of dilute- to densephase conditions (Figure 2), a two-layer based model for solids friction factor has been derived for straight pipe loss (Setia et al. 2016). Along with this common straight pipe model, five different bend models were applied to calculate the total pipeline pneumatic conveying characteristics using a MS EXCEL-based program containing different straight pipeline sections and bends. Subsequently, the predicted total pipeline pneumatic conveying characteristics were compared with the experimental plots to evaluate the influence of selection of bend model on the total pipeline pressure drop. The two-layer model for solids friction through straight pipe is provided by Equation (20).

$$k_s \frac14 s_1 8:04\, ðVLRÞ_{0:22}ðw_{fo}=V_fÞ_{1:48}$$
$$\flat s_2 0:0043\, \left[C=V_f \flat 2ðw_{f0}=V_fÞ \right] = \frac12 ðC=V_f Þ\, Fr^2 \qquad (20)$$

where

VLR ðvolumtric loading ratioÞ $\frac14$ ðm$_s$=q$_s$Þ=m$_f$ =q$_f$

$$(21)$$

K, a, b are constant and exponents of power function format and s_1 and s_2 represent the relative contributions of nonsuspension and suspension layers, respectively, based on the Froude number criteria. The first term in Equation (20), s_1 (K (VLR)^a (w$_{fo}$/V$_f$)^b), represents the solids friction contribution of the non-suspension flow, whereas the second term,
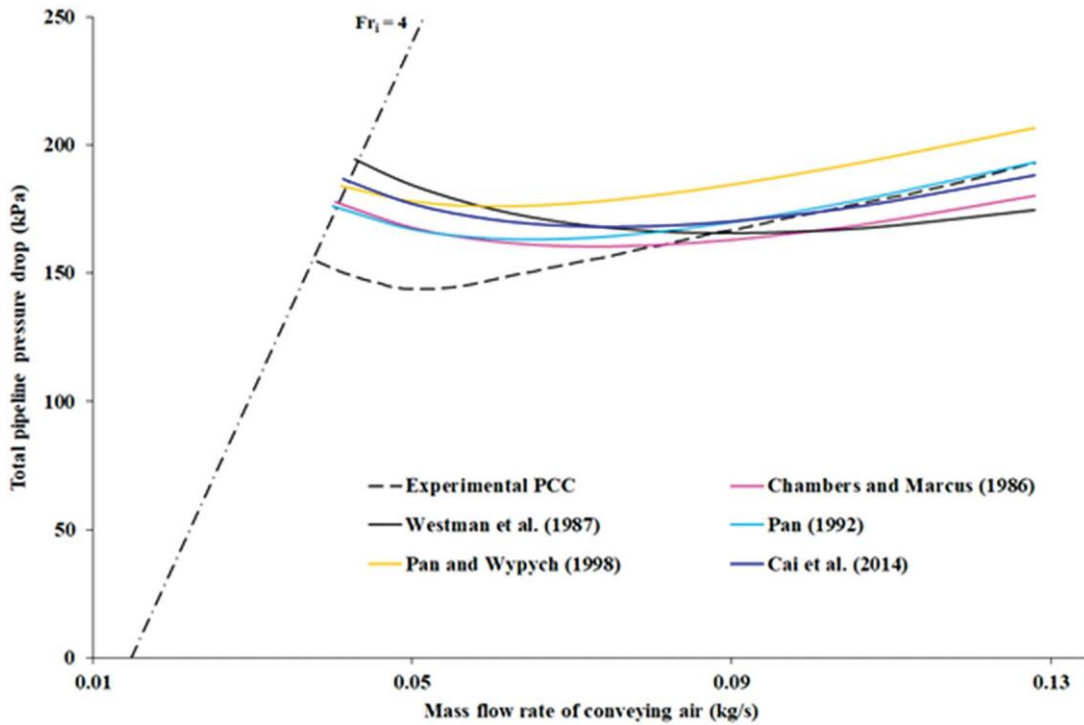
s2 (ksC/Vf þ 2 wf0/Vf/[(C/Vf) Fr2]), represents the suspension flow contribution. From a knowledge of ks, the pressure loss for a straight horizontal section of pipe for the solidsgas mixture can be calculated using Equation (22), as given by Barth (1954). The straight-pipe model format of Setia et al. (2016) was proposed after a comprehensive validation for fly ash, ESP dust and cement conveyed through 69 and 105 mm diameter and 168 m, 407 m and 554 m long pipelines. Qingliang et al. (2017) independently validated the accuracy of the two-layer modeling procedure of Setia et al. (2016) and found reliable agreements with experimental data.

$$Dp ¼ ðk_f þ m \ k_sÞ:L=D : q:V_f^2=2D \quad (22)$$

The effect of selecting a particular bend model on the prediction of total system pressure loss was evaluated by estimating the total pipeline conveying characteristics for fly ash for different solids throughput ranges for the 69 mm I.D. 168 m and 105 mm I.D. 168 m long test rigs by using several of the existing bend models separately and comparing the predicted PCC thus obtained (with themselves and with the experimental PCC). Losses due to initial acceleration and vertical pipe were estimated as per Chambers and Marcus (1986) as given by Equations (23) and (24), respectively. Equations (20–22) were used to estimate the straight pipe pressure drop.

$$\text{Acceleration loss: } Dp_{accel} ¼ q_f V^21 þ 2mC=V_f =2 \quad (23)$$

$$\text{Vertical loss: } Dp_V ¼ m \ q_f gL_vV_f =C \quad (24)$$

Since the same set of models were used to estimate losses occurring in horizontal pipe lengths, verticals and for initial acceleration and that the straight-pipe model is a validated reliable model (Setia et al. 2016; Qingliang et al. 2017), therefore any variation in magnitude (and trend) of the predicted total pipeline pneumatic conveying characteristics should occur only because of the choice of different bend models. Results are shown in Figures 5 and 6 for 69 mm I.D. and 168 m long pipeline for 19 t/h of ash flow rate and 105 mm I.D. and 168 m long pipeline for 28 t/h ash flow rate, respectively.

The above comparison plots show that the selection of different bend models can generate significantly different predicted conveying characteristics (even though they all use the same solids friction factor model to calculate pressure drop in straight horizontal runs). The Westman, Michaelides, and Thomson (1987) model has generated large over-prediction in dense-phase region and the predicted trends did not comply with the trends of experimental plots. Pan and Wypych (1998) model has provided desirable (but somewhat over-predicted) trends for both the pipelines. Perhaps this is because this model was developed specifically using fly ash data. The Chunhui et al. (2012) model provided large over-predictions, hence predictions using the same have not been included in Figures 5 and 6.

5. Development of new bend loss model

An empirical model for solids friction in bends has been developed using the experimental data of 209 experiments covering 3 products, 2 bend or pipeline diameter, 3 radius of curvature and 2 locations of test bend using sum of least square method. Table 5 lists the range of velocity values (before and after the bends) adopted in the experimental

Figure 6. Comparison of experimental and predicted values of the total pressure drop using different bend models in a pipeline (fly ash, D ¼ 105 mm, L ¼ 168 m,
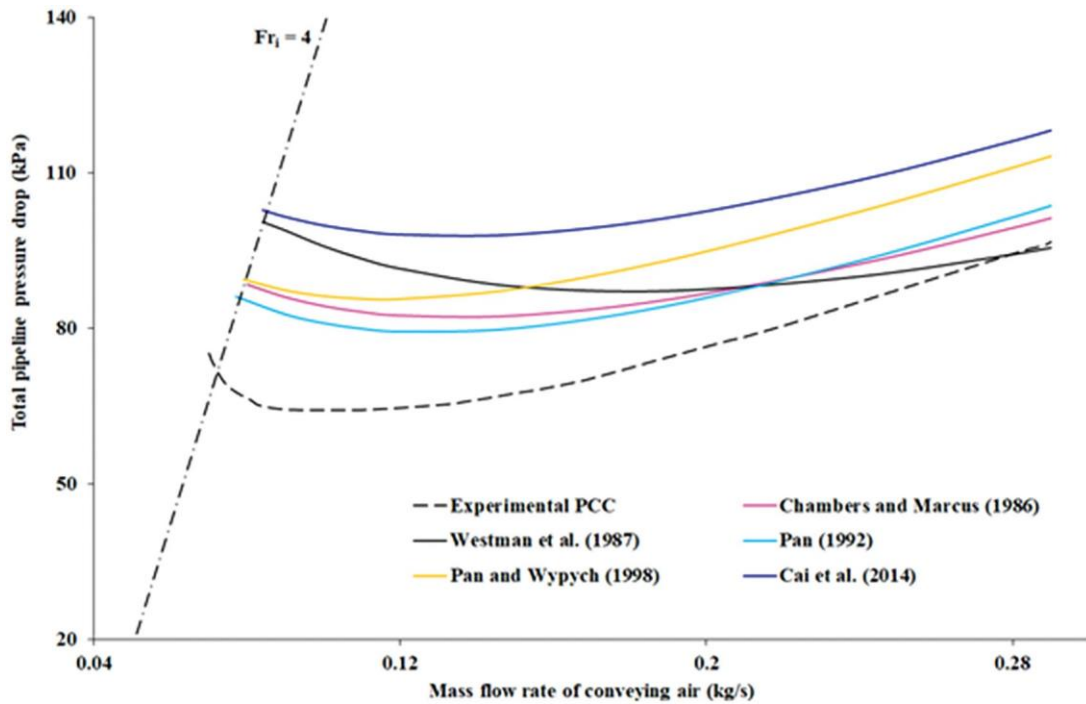
$m_s \approx 28$ t/h).

program from where a new bend loss model has been generated. Table 4 only lists the upper and lower ranges of velocities and loading ratio. Model for pressure drop through bend was using the test data of 209 number of experiments and is given by Equations (24) and (25). Air density and velocity values used in the model correspond to that of exit to the bend. The ratio of air density term in the model addresses the location of bends in the pipeline (air density decreases in the direction of flow). The R_b/D term describes the effect of radius of curvature of bend. The d_{50}/D term addresses the particle size effect on solids friction through the bend. The gas Froude number term describes the effect of conveying velocity on the particle-particle-wall friction at the bend.

$$\Delta p_b = \left(k_{bf} + m k_{bs}\right) \frac{\rho_{fo} V_{fo}^2}{2} \quad (25)$$

$$k_{bs} = 0.215 \left(\frac{\rho_f}{\rho_b}\right)^{0.86} \left(\frac{R_b}{D}\right)^{-0.246} \left(\frac{d_{50}}{D}\right)^{0.189} (Fr)^{-0.38} \quad (26)$$

Referring to Equation (26), negative exponent value of the ratio of gas density to powder bulk density indicates that as the bulk density of product increases, there would be more solids friction in bends. Negative exponent value of the ratio of radius of curvature of bend to pipe diameter indicates that for sharper bends, the solids friction through the bend would be more. Positive exponent value of the ratio of median particle diameter to pipe diameter indicates that for larger

particles, the solids friction through the bend would be more. Negative exponent value of Froude number indicates that when the gas velocity is high, the solids friction through the bend would be less due to reduced particle-particle contact.

Table 5. Ranges of air velocity values before and after the bend.

Case	m_f (kg=m³)	m_s (kg=m³)	m	V_i (m=s)	V_o (m=s)
1	0.057	0.33	5.8	15.7	15.8
	0.037	1.99	53.2	7.6	7.6
2	0.054	0.51	9.5	14.0	14.1
	0.042	2.24	54.0	8.8	8.9
3	0.042	1.62	38.6	8.9	9.0
	0.040	2.15	54.4	8.1	8.2
4	0.042	1.59	38.2	11.1	11.2
	0.039	2.09	53.1	10.2	10.2
5	0.045	0.56	12.6	11.8	11.9
	0.034	2.16	63.6	7.1	7.1
6	0.047	1.23	26.3	10.5	10.7
	0.040	2.03	50.9	8.2	8.2
7	0.058	0.35	6.0	20.3	20.4
	0.047	1.07	22.7	14.6	14.7

While several of the existing models were developed from limited experimental conditions, the new model (Equation (26)) has been developed from three product data, two pipeline or bend diameters, three different radius of curvatures and two different locations of test bend in the pilot plant. Hence, the new model can be expected to be useful for a large number of cases of fine powder conveying, pipeline and bend configurations. It should be noted that in several existing models for bend pressure drop, the V^2 term has been only used to represent the basic framework in the existing models (just as V^2 term has been included in Darcy formula for air-only fluid). Therefore, with both V^2 and k_{bs} in use,

the effective exponent of velocity term (using Froude number term) has not been 2. Figure 7 shows a comparison of the solids friction through bends predicted using equation 25 versus the experimental finding. The standard deviation error is 0.51 kPa and the average error is 0.50 kPa.

Figures 8 and 9 show the relative magnitudes of straight pipe to bend losses for the 69 mm I.D and 168 m long
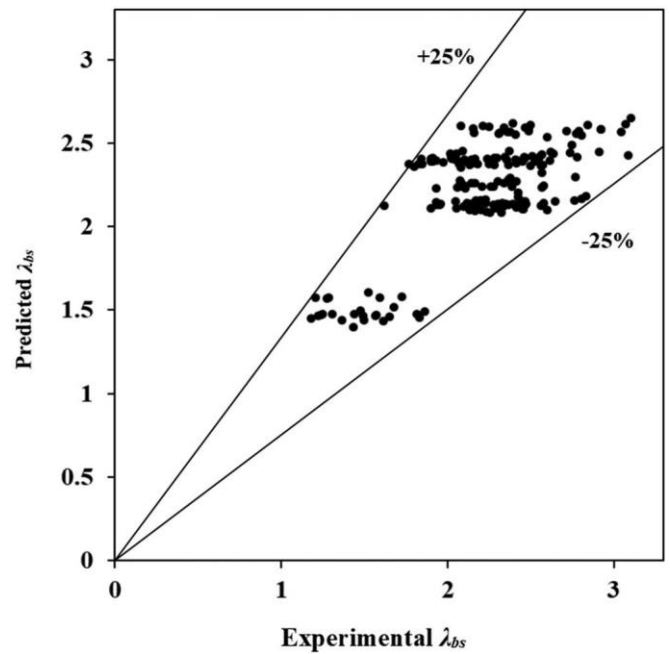

Figure 7. Experimental versus predicted values of solids friction factor through bends.

pipeline and 105 mm I.D and 168 m long pipelines for ash flow rates of 19 t/h and 28 t/h, respectively for different existing models (developed by other researchers) and that developed by the authors in this paper (given by "Author model"). Relative magnitudes have been reported in terms of percentage of total pipeline pressure drop. Losses due to verticals and initial acceleration (where the product is being fed into the pipeline by the blow tank) have been clubbed into the straight-pipe loss category.

A comparison of Figures 8 and 9 shows that the percentage losses in the bends are more in case of the larger diameter pipe (i.e. the percentage of bend losses are more the 105 mm I.D. pipeline compared to the 69 mm pipe I.D.). Although, the predicted straight pipe losses are less in the larger diameter pipeline, the relative magnitude of losses in bends are significantly larger compared to smaller diameter pipes (for the same number of bends). This validates that the mechanism of frictional losses in bends and straight pipes are quite different. Whereas all the models have shown an increase in pressure drop in bends with an increase in air flow rates, the bend loss predictions obtained using Westman, Michaelides, and Thomson (1987) model show a
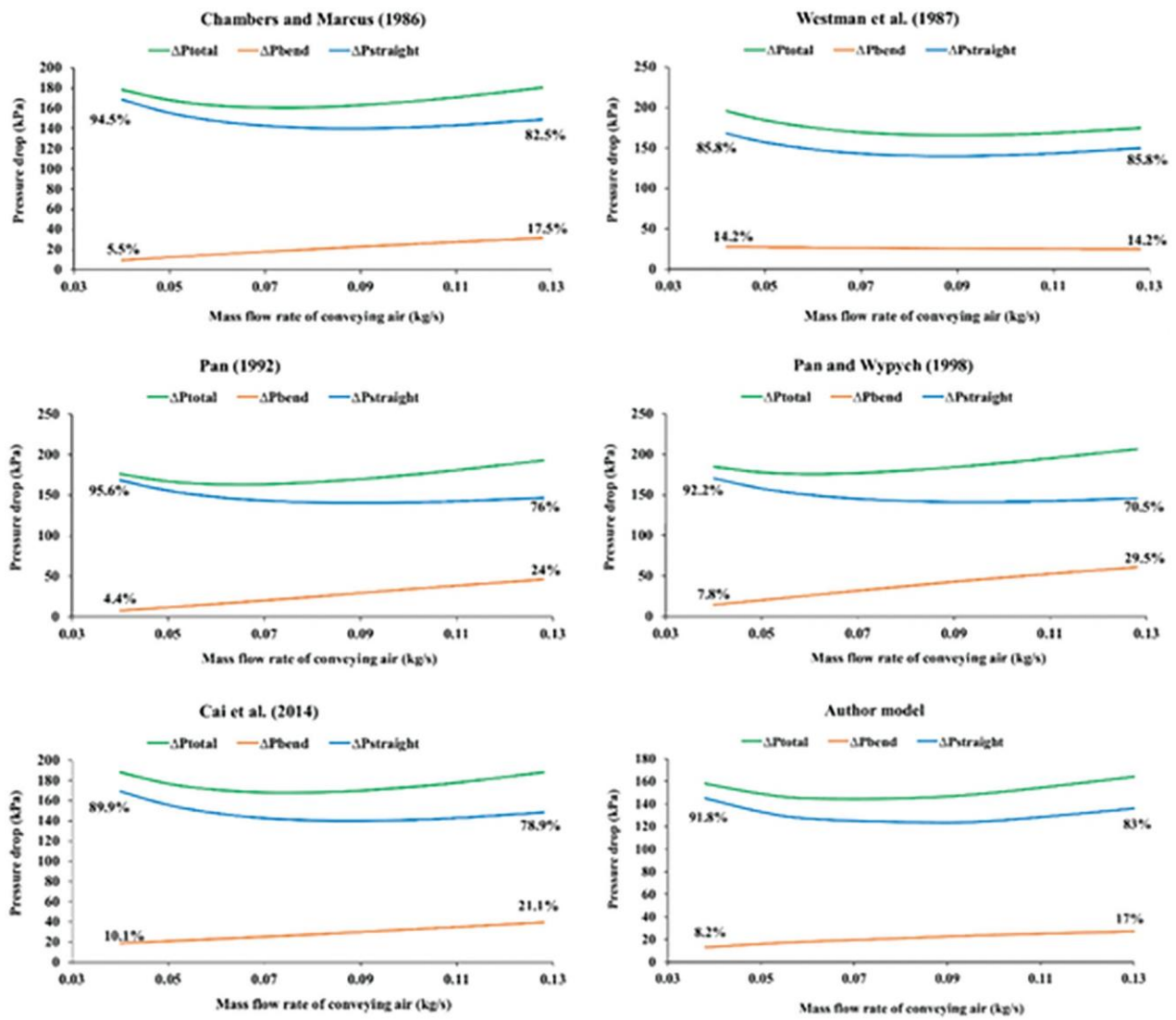
Figure 8. Trends of pressure drops in straight pipes versus bends predicted using different bend loss models (fly ash, D ¼ 69 mm, L ¼ 168 m, m$_s$ ¼ 19 t/h).
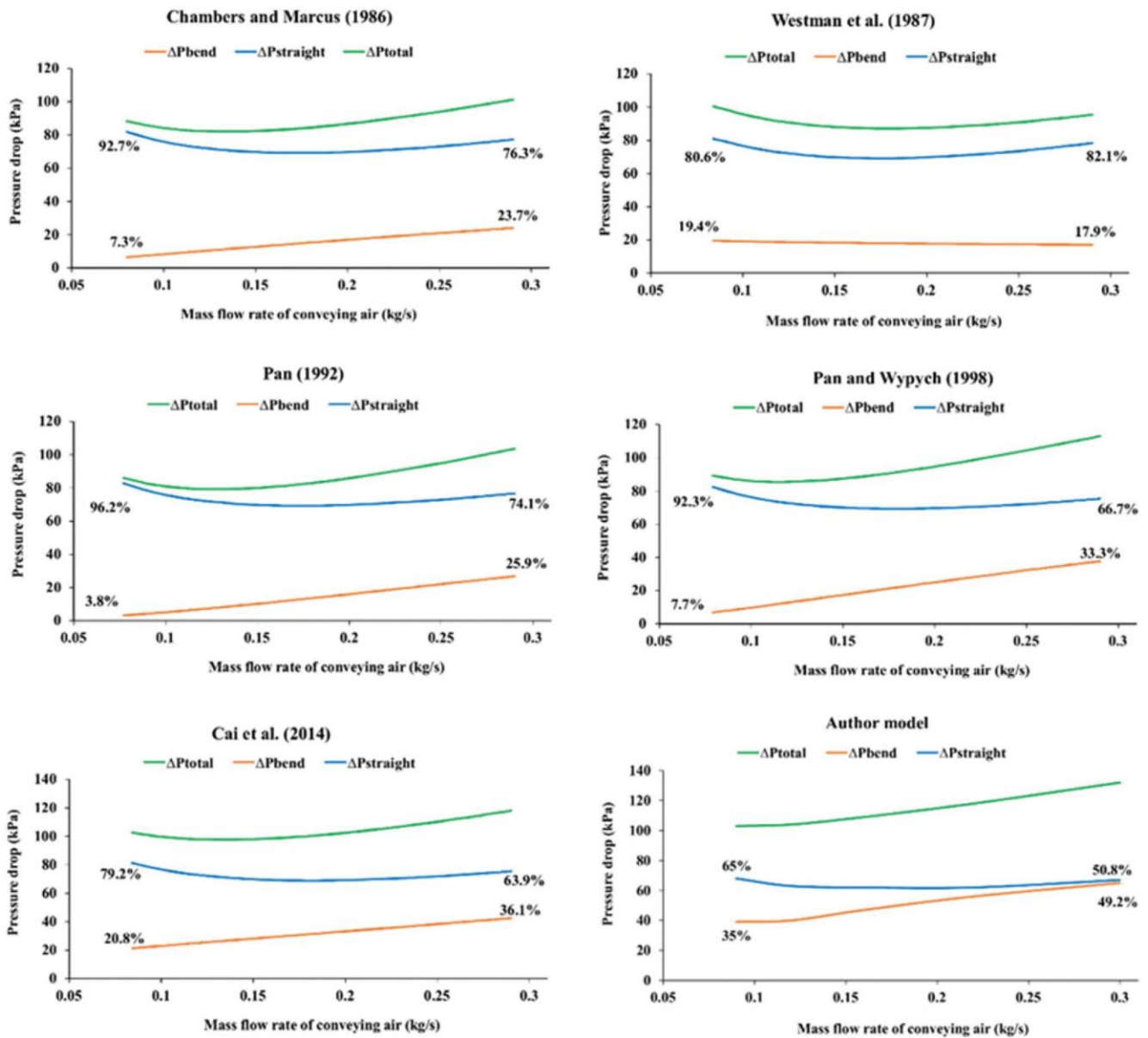
Figure 9. Trends of pressure drops in straight pipes versus bends predicted using different bend loss models (fly ash, D ¼ 105 mm, L ¼ 168 m, m$_s$ ¼ 28 t/h).

different trend. Westman, Michaelides, and Thomson (1987) model provides almost same prediction in dense and dilutephase. Except the Westman, Michaelides, and Thomson (1987) model (which shows a trend contrary to all other models), the range of predicted bend loss in dense-phase varies from 4.4 to 10.1%, whereas the same in dilute-phase varies from 17 to 29.5% for the 69 mm I.D and 168 m long pipeline; similar values in the 105 mm I.D and 168 m long pipeline for the dense and dilute-phases are 3.8 to 35% and 23.7 to 49.2%, respectively. It is evident that the differences in range of predictions get enhanced with an increase in pipe diameter.

6. Conclusions

The estimation of bend pressure drop can have a considerable impact on correctly predicting the total pressure loss in a

pneumatic conveying system. The predicted pneumatic conveying characteristics obtained using three different bend models are found to be significantly different, in terms of both predicted values and overall trends, thus signifying the requirement of correctly selecting an appropriate bend model towards reliably predicting total pipeline pressure drop. A new bend loss model has been developed based on the conveying data of gray cement, fly ash and white cement, conveyed through 42 and 53 mm bend diameter, radius of curvatures of 1000, 800 and 600 mm and having two different test bend locations. Out of 209 experiments, 120 experiments had different values of ratio of radius of curvature of bend to pipe diameter. The new model is applicable for fluidized dense-phase type conveying of Geldart Group A type fine powders. Practical installations involve losses due to the bends and the derived model for bend loss can be used to predict such losses for a range of fine powders, pipeline

diameters and radius of curvature of bends, as the model involves physical properties of particles, pipelines and bends. It is expected that certain type of fine powders, such as fly ash, would gain more fluidity (better flowability) associated with reduced pressure drop. Humidity would in general cause lack of flowability (even pipeline blockage), especially if the powders are hygroscopic. The new model incorporates the effects of gas velocity, pipe diameter, particle diameter, bulk density of powders and radius of curvature of bends. As this model covers a range of properties of powders, pipeline, bend and conveying conditions, the developed model could be useful to predict bend loss for a large number of industrial cases. Future scope of work would involve validation of the developed bend model for larger diameter pipelines.

Acknowledgement

Disclosure statement

List of symbols

a_b	Constant in Singh and Wolf equation
a_c	Bend pressure loss under air-only conditions in Singh and Wolf equation [kPa]
a_s	Constant in Singh and Wolf equation
B	Bend constant in Chambers–Marcus equation
C	Particle velocity [m/s]
D	Internal diameter of pipe [m]
d_p	Median particle diameter [mm]
e	the natural constant, e ¼ 2.718 Froude
Fr ¼ V_f =ð ÞgD $^{0:5}$	number of flow
g	Acceleration due to gravity [m/s²]
L	Total length of the pipe [m]
L_v	Length of the vertical pipe [m]
m_a	Mass flow rate of air [kg/s]
m_s	Mass flow rate of solids [kg/s]
m ¼ m_s=m_a Dp	Solids loading ratio
	Pressure drop through a straight horizontal pipe or pipe section [kPa]
Dp_b	Pressure drop due to solid-air mixture through bend [kPa]
Dp_{bs}	Solids contribution to the pressure drop through a bend [kPa]
Dp_{zs}	Solids contribution to the pressure drop through a straight pipe [kPa]
DP_{accel}	Pressure drop due to initial acceleration [kPa]
DP_v	Pressure drop due to the verticals [kPa]
R_b	Radius of curvature of bend [m]
Re	Reynolds number
V_f	Superficial air or gas velocity [m/s]
V_0	Superficial air or gas velocity at bend outlet [m/s]

w_{fo}	Terminal settling velocity [m/s]

Greek symbols

k_{bf}	Air alone friction factor through bend
k_{bs}	Friction factor due to solids through bend
q_f , q_a	Fluid or air density [kg/m³]
q_b	Loose-poured bulk density [kg/m³]
q_p, q_s	Particle density [kg/m³]

Acronym

ID	Internal Diameter

Subscripts

b	Bend
o	Value at outlet of bend
f	Fluid

References

Akilli, H., E. K. Levy, and B. Sahin. 2001. Gas-solid flow behavior in a horizontal pipe after a 90 vertical-to-horizontal elbow. Powder Technology 116 (1):43–52. doi:10.1016/S0032-5910(00)00360-0.

Barth, W. 1954. Stromungstechnische Probleme Der Verfahrenstechnik.€ Chemie Ingenieur Technik 26 (1):29–34. doi:10.1002/cite.330260108.

Bilirgen, H., and E. K. Levy. 2001. Mixing and dispersion of particle ropes in lean phase pneumatic conveying. Powder Technology 119 (2–3):134–52. doi:10.1016/S0032-5910(00)00413-7.

Cai, L., S. Liu, X. Pan, X. Guiling, Y. Gaoyang, C. Xiaoping, and Z. Changsui. 2014. Comparison of pressure drops through different bends in dense-phase pneumatic conveying system at high pressure. Experimental Thermal and Fluid Science 57:11–9. doi:10.1016/j.expthermflusci.2014.03.016.

Chambers, A. J., and R. D. Marcus. 1986. Pneumatic conveying calculations. Paper presented at the Second International Conference on Bulk Materials Storage, Handling and Transportation: 1986; Preprints of Papers, 49. Institution of Engineers, Australia.

Chunhui, H., C. Xianmei, W. Jianhao, N. Hongliang, X. Yupeng, Z. Haijun, X. Yuanquan, and S. Xianglin. 2012. Conveying characteristics and resistance characteristics in dense phase pneumatic conveying of rice husk and blendings of rice husk and coal at high pressure. Powder Technology 227:51–60.

Crowe, C. T., ed. 2005. Multiphase flow handbook. 1st ed. Boca Raton: CRC Press.

Das, P. K., and J. R. Meloy. 2002. Effect of close-coupled bends in pneumatic conveying. Particulate Science and Technology 20 (4): 253–66.

Hall, S. 2012. Rules of thumb for chemical engineers. 5th ed. Oxford: Butterworth-Heinemann.

Hastie, D. B., R. Pan, P. W. Wypych, and P. R. Guiney. 2001. Handbook of conveying and handling of particulate solids. Handbook of Powder Technology 10:379–86.

Hettiaratchi, K., S. R. Woodhead, and A. R. Reed. 1998. Comparison between pressure drop in horizontal and vertical pneumatic conveying pipelines. Powder Technology 95 (1):67–73. doi:10.1016/S00325910(97)03318-4.

Hyder, L. M., M. S. A. Bradley, A. R. Reed, and K. Hettiaratchi. 2000. An investigation into the effect of particle size on straight-pipe pressure gradients in lean-phase conveying. Powder Technology 112 (3): 235–43. doi:10.1016/S0032-5910(00)00297-7.

Klinzing, G. E., F. Rizk, R. Marcus, and L. S. Leung. 2010. Pneumatic conveying of solids: A theoretical and practical approach. 3rd ed. New York: Springer.

Levy, A., and D. J. Mason. 1998. The effect of a bend on the particle cross-section concentration and segregation in pneumatic conveying systems. Powder Technology 98 (2):95–103. doi:10.1016/S00325910(97)03385-8.

Mallick, S. S. 2009. Modelling dense-phase pneumatic conveying of powders. PhD Diss., University of Wollongong, Australia. Maynard, E. 2006. Designing pneumatic conveying systems. Chemical Engineering Progress 102:23–33.

McGlinchey, D., ed. 2008. Bulk solids handling: Equipment selection and operation. 1st ed. Oxford: Blackwell Publishing Ltd. Molerus, O. 1996. Overview: Pneumatic transport of solids. Powder Technology 88 (3):309–21. doi:10.1016/S0032-5910(96)03136-1.

Pan, R. 1992. Improving scale-up procedures for the design of pneumatic conveying systems. PhD. Diss., University of Wollongong, Australia.

Pan, R., and P. W. Wypych. 1998. Dilute and dense phase pneumatic conveying of fly ash. Paper presented at the Proceedings of the 6th International Conference on Bulk Materials Storage and Transportation, Wollongong, NSW, Australia, 183–9.

Qingliang, G., L. Zhen, F. Xinhui, L. Bing, P. Baozai, F. Ziyang, S. Ya, and L. Wenhua. 2017. Experimental study on dense-phase pneumatic conveying of coal powder at high pressures. Clean Energy 1 (1):50–67. doi:10.1093/ce/zkx007.

Rossetti, S. J. 1983. Concepts and criteria for gas-solids flow. Handbook of fluids in motion. Boston: Ann Arbor Science Publishers.

Schuchart, P. 1968. Widerstandsgesetze beim pneumatischen transport in Rohrkrummern.€ Chemie Ingenieur Technik 40 (21–22):1060–7. doi:10.1002/cite.330402107.

Setia, G., S. S. Mallick, P. W. Wypych, and R. Pan. 2016. Modeling solids friction factor for fluidized dense-phase pneumatic transport of powders using two-layer flow theory. Powder Technology 294:80–92. doi:10.1016/j.powtec.2016.02.006.

Singh, B., and R. R. Wolfe. 1972. Pressure losses due to bends in pneumatic forage handling. Transactions of the ASAE 15 (2):246–8.

Tripathi, N. M., A. Levy, and H. Kalman. 2018. Acceleration pressure drop analysis in horizontal dilute phase pneumatic conveying system. Powder Technology 327:43–56. doi:10.1016/j.powtec.2017.12. 045.

Vasquez, N., K. Jacob, R. Cocco, S. Dhodapkar, and G. E. Klinzing. 2008. Visual analysis of particle bouncing and its effect on pressure drop in dilute phase pneumatic conveying. Powder Technology 179 (3):170–5. doi:10.1016/j.powtec.2007.06.015.

Venkatasubramanian, S., H. Tashiro, G. E. Klinzing, and K. Mykelbust. 2000. Solids flow behavior in bends: Assessing fine solids buildup. Powder Technology 113 (1–2):124–31. doi:10.1016/S0032-5910(00)00217-5.

Westman, M. A., E. E. Michaelides, and F. M. Thomson. 1987. Pressure losses due to bends in pneumatic conveying. Journal of Pipelines 7 (1):15–20.

Wypych, P. W. 1999. Pneumatic conveying of powders over long distances and at large capacities. Powder Technology 104 (3):278–86. doi:10.1016/S0032-5910(99)00105-9.

Yan, Y., B. Byrne, and J. Coulthard. 1994. Radiometric determination of dilute inhomogeneous solids loading in pneumatic conveying systems. Measurement Science and Technology 5 (2):110–9. doi:10.1088/ 0957-0233/5/2/006.